A neutron diffraction investigation of solutions of nickel in molten nickel iodide and molten nickel bromide

1991 J. Phys.: Condens. Matter 3 97

(http://iopscience.iop.org/0953-8984/3/1/008)

J. Phys.: Condens. Matter 3 (1991) 97–110. Printed in the UK

A neutron diffraction investigation of solutions of nickel in molten nickel iodide and molten nickel bromide

D A Allen and R A Howe
Department of Physics and Astronomy, University of Leicester, Leicester LE1 7RH, UK

Received 21 June 1990

Abstract. The short-range chemical order of solutions of nickel in molten $NiBr_2$ and NiI_2 at 9 mol% concentration has been investigated by neutron diffraction. By using isotopically enriched samples, the three partial structure factors for $NiBr_2$ + Ni have been determined by measurements made using the steady-state reactor source at the Institute Laue–Langevin. For NiI_2 + Ni, the partial structure factor relating to I–I correlations has been determined and information on the other two structure factors has been obtained by the time-of-flight method using the intense pulsed neutron source at Argonne National Laboratory. The results are compared with those of previous diffraction studies of the pure salts. No evidence for the formation of subhalide complex ions has been found. It is proposed that nickel dissolves according to the equation $Ni \rightarrow Ni^{2+} + 2e^-$, with the excess nickel ions occupying tetrahedrally coordinated sites within the liquid structure indistinguishable from those in the pure salt.

1. Introduction

The nature of mixtures of metals with their molten salts has long been of interest to chemists and it was established in the late 1950s that true solutions, rather than colloidal dispersions, are indeed formed (Bredig and Johnson 1960). Two categories of metal–molten salt solutions have been identified (see, e.g., Nachtrieb 1974).

(i) Those in which the added metal imparts metallic behaviour to the solution. Members of this class of solution exhibit mixed ionic and electronic conduction even at low metal concentrations and include most of the alkali metal–alkali halide solutions.

(ii) Those for which the electrical conductance and its temperature coefficient are typical of ionic solutions. There is no significant increase in the conductivity of these salts upon dissolution of metal. This class of solutions includes many polyvalent metals in their halides such as Bi halides, Hg halides and alkaline-earth halides.

For this second class of metal–molten salt mixtures, the lack of an electronic contribution to the conductivity at the salt-rich end of the composition range is usually attributed to the removal of conduction electrons by the formation of cationic species of lower oxidation states than those found in the pure salt. Mixtures of this category are often designated 'subhalide' solutions. A number of polyatomic species have been proposed including Na_2 in Na–NaBr, Cd_2^{2+} in Cd–$CdCl_2$ and even larger complexes such as Bi_4^{4+} or Bi_9^{5+} in Bi–Bi halide melts. However, very little structural data exists for polyvalent metals in their molten salts. In this paper, results are presented of neutron

0953-8984/91/010097 + 14 $03.50

diffraction investigations of the structures of solutions of NiI_2 + 9 mol% Ni and $NiBr_2$ + 9 mol% Ni.

Previous neutron diffraction studies of the pure salts $NiCl_2$, $NiBr_2$ and NiI_2 have been reported by Newport *et al* (1985), Wood and Howe (1988) (hereafter referred to as I) and Wood *et al* (1988) (hereafter referred to as II). The favourable conditioning for the separation of partial structure factors that is obtained by the isotopic substitution of the nickel species has been exploited, and the three partial structure factors have been obtained to a high degree of accuracy for all three salts. All of these molten halides possess a closely packed anion structure, which is remarkably similar throughout the series, with nickel ions occupying tetrahedrally coordinated sites within this structure. It was the aim of the experiments reported in this paper to investigate the nature of the dissolved metal in Ni + Ni halide solutions—in particular whether subhalide species are formed. Nickel isotopic substitution has again been used to obtain two total structure factors for NiI_2 + 9 mol% Ni using both natural and 'zero' nickel (an isotopic mix of nickel having a coherent scattering length of zero), and the three partial structure factors for $NiBr_2$ + 9 mol% Ni.

2. Experimental details

The quantity which can be determined from a single neutron diffraction experiment on a liquid containing two atomic species a and b in concentrations C_a and C_b is the total structure factor $F(Q)$. Using the Faber–Ziman definition this is defined by

$$F(Q) = C_a^2 b_a^2[S_{aa}(Q) - 1] + C_b^2 b_b^2[S_{bb}(Q) - 1] + 2C_a C_b b_a b_b[S_{ab}(Q) - 1] \tag{1}$$

where b_a and b_b are the coherent neutron scattering lengths of the two species and S_{aa}, S_{bb} and S_{ab} are the partial structure factors. These can be related to the pair distribution functions $g_{\alpha\beta}(r)$ by Fourier sine transformation

$$S_{\alpha\beta}(Q) = 1 + \frac{4\pi\rho}{Q}\int_0^\infty [g_{\alpha\beta}(r) - 1]r \sin(Qr)\,dr \tag{2}$$

where $\alpha, \beta \equiv$ a or b and ρ is the mean atomic number density.

To extract the three partial structure factors for $NiBr_2$ + 9 mol% Ni, the neutron scattering intensity was measured for three samples in which the isotopic abundances of nickel, and hence the coherent scattering lengths b_{Ni}, were different. For NiI_2 + 9 mol% Ni, the partial structure factor S_{II}, was extracted and information on the other two partial structure factors was obtained, as a linear combination of S_{NiNi} and S_{NiI}, by measuring the neutron scattering intensity from two samples with different isotopic abundances of nickel. Table 1 lists the chemical and isotopic compositions of all five samples, together with the neutron scattering and sample size parameters used for the data analysis.

The isotopically enriched mixtures were prepared in powdered form by the isotopic preparation unit at the University of Bristol. These were dried by the method described by Newport *et al* (1985) and melted for 10 h. The final samples were sealed in fused quartz containers with a nominal wall thickness of 1 mm. The natural mixtures were prepared by melting the pure dried salts with a weighed quantity of nickel wire for a period of 15 h prior to sealing in their final sample tubes.

The time-of-flight neutron scattering experiment for NiI_2 + Ni was undertaken on the general-purpose powder diffractometer at the intense pulsed neutron source,

Table 1. The isotopic compositions and nickel concentrations of the five isotropically enriched samples, and the parameters used for the data analysis.

	Natural $NiI_2 + Ni$	'Zero' $NiI_2 + Ni$	Natural $NiBr_2 + Ni$	'Zero' $NiBr_2 + Ni$	$^{62}NiBr_2 + Ni$
Amount of added Ni (mol%)	8.9 ± 0.3	8.27 ± 0.10	9.01 ± 0.10	9.01 ± 0.10	8.97 ± 0.10
Amount of natural Ni (%)	35.26	1.81	35.46	1.84	1.17
Amount of ^{60}Ni (%)	0	23.54	0	23.72	0
Amount of ^{62}Ni (%)	0	9.76	0	9.89	34.28
Amount of anion (%)	64.74	64.88	64.54	64.54	64.55
Coherent scattering lengths† (10^{-12} cm)					
$\bar{b}_{Ni}$	1.03	0	1.03	0	−0.807
$\bar{b}_{anion}$	0.528		0.679		
Scattering cross sections† (b)					
σ^{inc}	2.56	2.31	2.25	2.9	6.98
σ^{abs}	5.59	6.22	2.38	2.62	3.74
Sample radius (mm)	4.23	4.23	3.85	3.84	3.84
Density (g cm^{-3})	4.37		3.88		

† From Sears (1984).

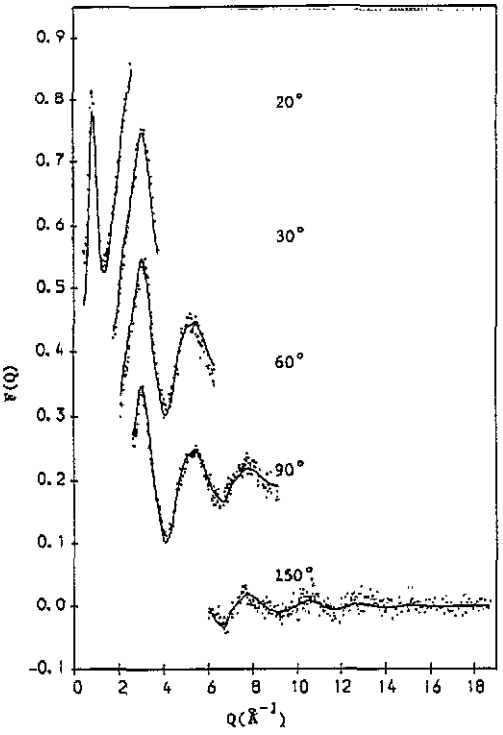

Figure 1. The total structure factor of natural NiI_2+ 9 mol% Ni. $F(Q)$ is shown for each detector bank over the range which contributes to the final $F(Q)$ and each successive curve is displaced by 0.2. The agreement between the different detector banks can be seen by comparison with the full curve, which is the back transform of a smoothed $G(r)$.

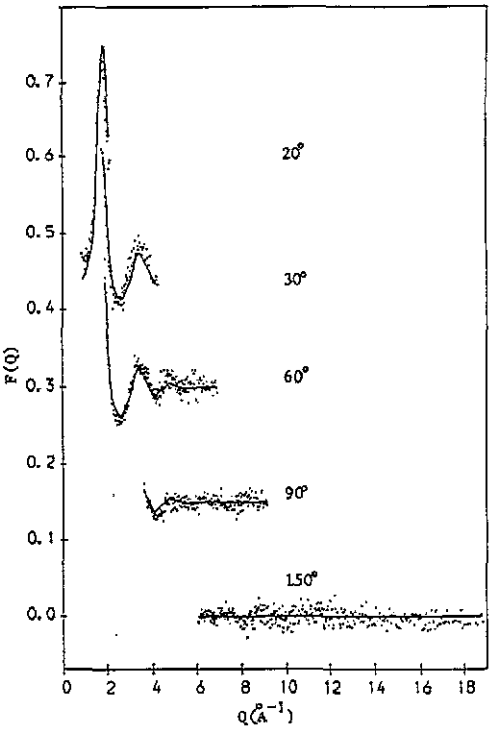

Figure 2. The total structure factor of 'zero' NiI_2 + 9 mol% Ni shown separately for each detector angle (●): ——, from the smoothed $g_{II}(r)$ and enables comparison between the different detector angles. Successive curves are displaced by 0.15.

Argonne National Laboratory (ANL). This is the same instrument that was used in II to determine the structure of pure NiI_2. The samples were heated by a vanadium foil furnace to 825 °C, some 30 °C above the melting point of the pure salt. The neutron beam height was 32 mm and data were collected simultaneously by ten groups of detectors at scattering angles of ±20°, ±30°, ±60°, ±90° and ±150° for a period of about two days per sample. Time focusing corrections were made for each detector and data from detector groups at positive and negative angles were analysed separately. Corrections were applied for sample and container attenuation and multiple, incoherent, background and container scattering by the method described by Howells (1986). The scattering from a vanadium rod 6.4 mm in diameter was used to normalize the spectra and the resulting contributions to the total structure factors for the different detector groups for both samples are shown in figures 1 and 2. The positive- and negative-angle detector groups showed good agreement and have been combined for these figures and for subsequent data analysis. No variation with time was observed for the diffraction from the two samples.

The steady-state diffraction experiment for $NiBr_2$ + Ni was caried out on the D4B diffractometer at the Institut Laue–Langevin (ILL) (1983), Grenoble, using neutrons

with a wavelength of 0.7 Å. Again this was the same instrument that was used to determine the structure of the pure salt in I. The samples were heated by a vanadium foil furnace to 995 °C, some 30 °C above the melting point of the pure salt, and the neutron beam height was set at 26 mm. In addition to the three samples, spectra were measured for an empty container and the empty furnace, a 5 mm vanadium rod and the empty instrument. Corrections were made for sample and container attenuation and multiple, incoherent, background and container scattering. A Placzek correction for inelastic scattering was applied to the scattering from the vanadium rod, which was then used to normalize the data.

In the absence of any phase diagram information for the $NiBr_2$ + Ni system, another sample of $NiBr_2$ + 9 mol% Ni was prepared in exactly the same manner and chemically analysed for nickel content. The excess nickel, which was originally in the form of wire, was found to be dispersed throughout the sample in concentrations of between 7.4 and 9.2 mol%, the top of the sample being slightly deficient. This inhomogeneity is due either to incomplete mixing in the liquid phase or to partial precipitation of nickel metal upon cooling because of a limited solid state solubility.

The scattering from the molten samples was measured by two detector banks, which scanned through their angular ranges a total of seven times for each sample. Each scan was of approximately 2 h duration. A comparison of successive scans for the natural and ^{62}Ni samples revealed diffraction patterns that were changing with time, apparently arising from the initial inhomogeneity of the samples and the subsequent redissolving of the precipitated solute metal over a period of about 15 h. In order to obtain meaningful diffraction data from the time-varying results for the ^{62}Ni sample, a method of extrapolation to infinite time was employed. The differences between the raw data for the first scan and that of each successive scan were obtained and an estimate of the asymptotic behaviour with time was made. This was determined by plotting the magnitude of a particular feature in the difference spectra as a function of time and making an estimate of its asymptotic behaviour. The particular feature used was that resulting from two slightly different peaks, since the first peak in the diffraction pattern for the ^{62}Ni sample was shifting to lower Q as the nickel dissolved. Other features in these difference spectra were small by comparison and not much greater than the noise. The final three measured scans were extrapolated to what one would expect them to be after an infinite time, by adding to them the appropriate difference spectra that were necessary to bring the magnitude of this feature to its asymptotic limit. The final spectrum that was used for the data analysis was that obtained from a flux-weighted mean of these three extrapolated scans. The statistical quality of this spectrum was equivalent to that of one original scan. Although this process does of course leave some uncertainty in the final extrapolated scan, it should be noted that the differences between this scan and the measured seventh scan were less than the statistical noise levels of these scans.

For the natural sample, only very small changes were observed during the time of the final three scans; so these were combined to form a single diffraction pattern. The diffraction pattern for the 'zero' nickel sample showed very little change between the first and the final scans. For the data analysis the final four scans were used.

3. Results

In order to create a single total structure factor for each sample of NiI_2 + Ni, the data from the individual counter groups were combined to form the total structure factors

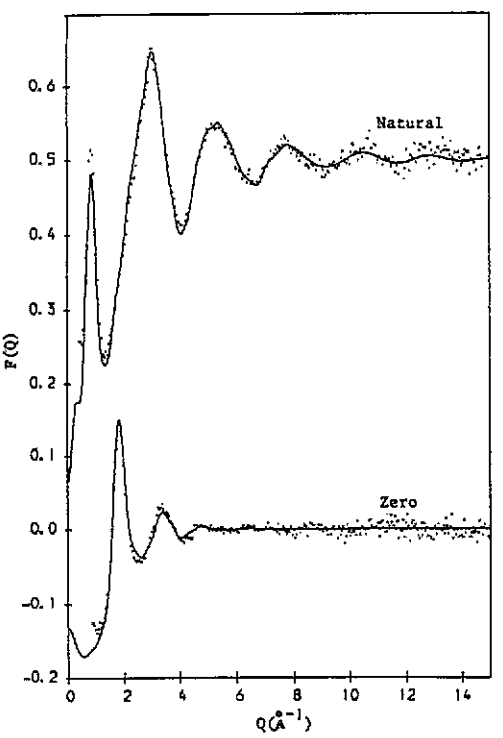

Figure 3. The total structure factors for natural and 'zero' NiI_2 + 9 mol% Ni obtained from a flux-weighted combination of the spectra from all of the detectors.

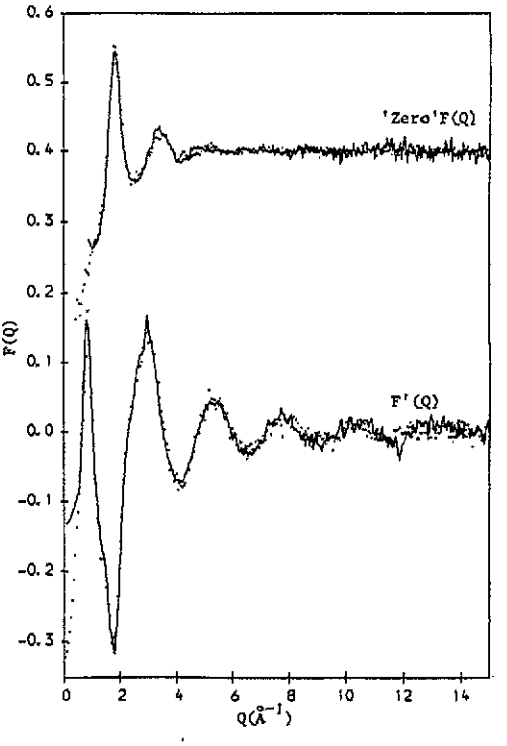

Figure 4. 'Zero' $F(Q)$ and $F'(Q)$ for NiI_2 + 9 mol% Ni (——) compared with the equivalent structure factors for the pure salt (●) (from II).

shown in figure 3. The ranges over which the data from the individual detector groups were included in the final $F(Q)$ were determined by comparison of the spectra, bearing in mind that at a given Q the neglected Placzek correction is least significant at small angles and high neutron energies. For consistency, these ranges were chosen to be the same for both samples. A flux-weighting method was used to combine the spectra and the data were binned into constant ΔQ intervals of 0.05 Å^{-1}. The agreement between the data from different counter groups can be seen in figures 1 and 2.

The two simultaneous equations for the $F(Q)$-values for this experiment derived from equation (1) are

$$^{zero}F(Q) = 0.117[S_{II}(Q) - 1] \tag{3}$$

$$^{nat}F(Q) = 0.116[S_{II}(Q) - 1] + 0.133[S_{NiNi}(Q) - 1] + 0.249[S_{NiI}(Q) - 1]. \tag{4}$$

The anion–anion partial structure factor is obtained directly from the 'zero' $F(Q)$ and, after a correction to take into account the slightly different nickel concentrations for the two samples, a combination $F'(Q)$ of the two other partial structure factors is obtained from a first-order difference of the two measured total structure factors:

$$F'(Q) = 0.133[S_{NiNi}(Q) - 1] + 0.249[S_{NiI}(Q) - 1]. \tag{5}$$

Figure 4 compares this function with the equivalent composite function for the pure salt.

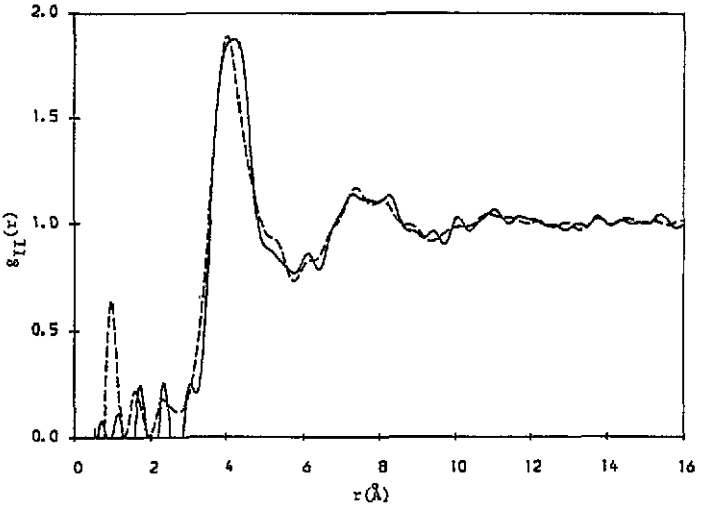

Figure 5. The I–I partial $g(r)$ for NiI_2 + 9 mol% Ni (——) compared with that of the pure salt (---) (from II).

The figure also shows the 'zero' $F(Q)$ for both the pure salt and the solution. In order to Fourier transform these structure factors it was necessary to extrapolate the data to $F(0)$. In the absence of any compressibility data for the salt and its mixtures with nickel, this limit was unknown. Fortunately the Fourier transform is relatively insensitive to this region of Q-space and uncertainty in the extrapolation was found to be of little consequence. Figure 5 compares the radial distribution function obtained upon transformation of $S_{II}(Q)$ with $g_{II}(r)$ for the pure salt.

For $NiBr_2$ + Ni, the data from the two counter banks on D4B showed excellent agreement over their regions of overlap and were combined using the same flux-weighting method and binned into constant ΔQ intervals of 0.025 $Å^{-1}$. Figure 6 shows the resulting total structure factors for the three samples. The three simultaneous equations for the total structure factors for this experiment are

$$^{zero}F(Q) = 0.192[S_{BrBr}(Q) - 1] \tag{6}$$

$$^{nat}F(Q) = 0.192[S_{BrBr}(Q) - 1] + 0.133[S_{NiNi}(Q) - 1] + 0.320[S_{NiBr}(Q) - 1] \tag{7}$$

$$^{62}F(Q) = 0.192[S_{BrBr}(Q) - 1] + 0.082[S_{NiNi}(Q) - 1] - 0.251[S_{NiBr}(Q) - 1]. \tag{8}$$

$S_{BrBr}(Q)$ is obtained directly from the 'zero' $F(Q)$, while the other two partial structure factors are separated by the second-order differencing of the three measured total structure factors. The partial structure factors are shown in figure 7. Again, the $F(0)$ limits have been estimated and chosen in a self consistent manner for the purposes of Fourier transformation. The results of the transforms are seen in figure 8, where they are compared with the distribution functions for the pure salt. The possible effect of uncertainty in the nickel concentration was investigated by analysing this data twice using two extremal models: first assuming a 9 mol% Ni solution and then assuming a pure salt. The main differences observed between the results for these two cases were to be found in $S_{NiNi}(Q)$, where the amplitude of the first main peak at $Q \simeq 2Å^{-1}$ was 27% greater when it was assumed that no excess nickel was present. This 27% difference

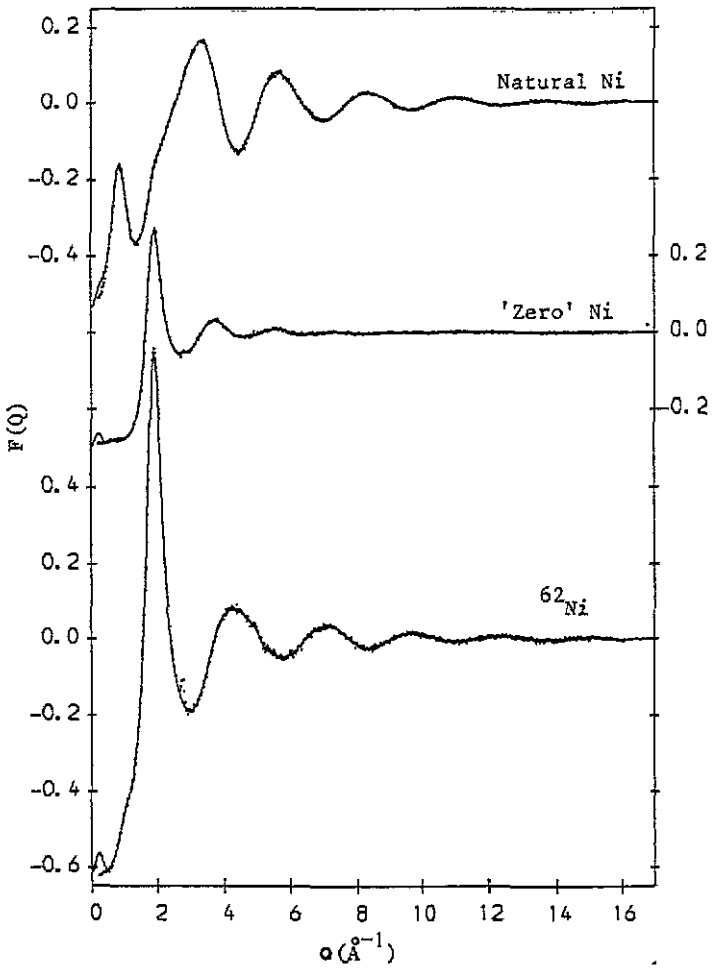

Figure 6. The total structure factors for the three isotopic samples of $NiBr_2$ + 9 mol% Ni (●): ——, obtained from the back transforms of the final partial distribution functions.

was small compared with that observed between the partial structure factors for the mixture and the pure salt. It was concluded therefore that, even with a small uncertainty in the concentration of the dissolved nickel and the added uncertainty introduced by the time dependence of the diffraction data, the observed changes in the structure factors of $NiBr_2$ upon addition of nickel metal are real and the structure factors presented here are representative of a 9 mol% Ni solution.

A summary of structural parameters for $NiBr_2$ + 9 mol% Ni and pure $NiBr_2$ is presented in table 2. The mean coordination number of β-atoms around an α-type atom was obtained by the method of integrating the function $r^2 g_{\alpha\beta}(r)$ up to its first minimum following the principal peak (Waseda 1980). The ratio $\bar{r}_{--}/\bar{r}_{+-}$ refers to the ratio of the peak positions in the functions $r^2 g_{BrBr}$ and $r^2 g_{NiBr}$ which, for a perfect tetrahedral arrangement of anions around each cation, should be $(8/3)^{1/2} = 1.633$.

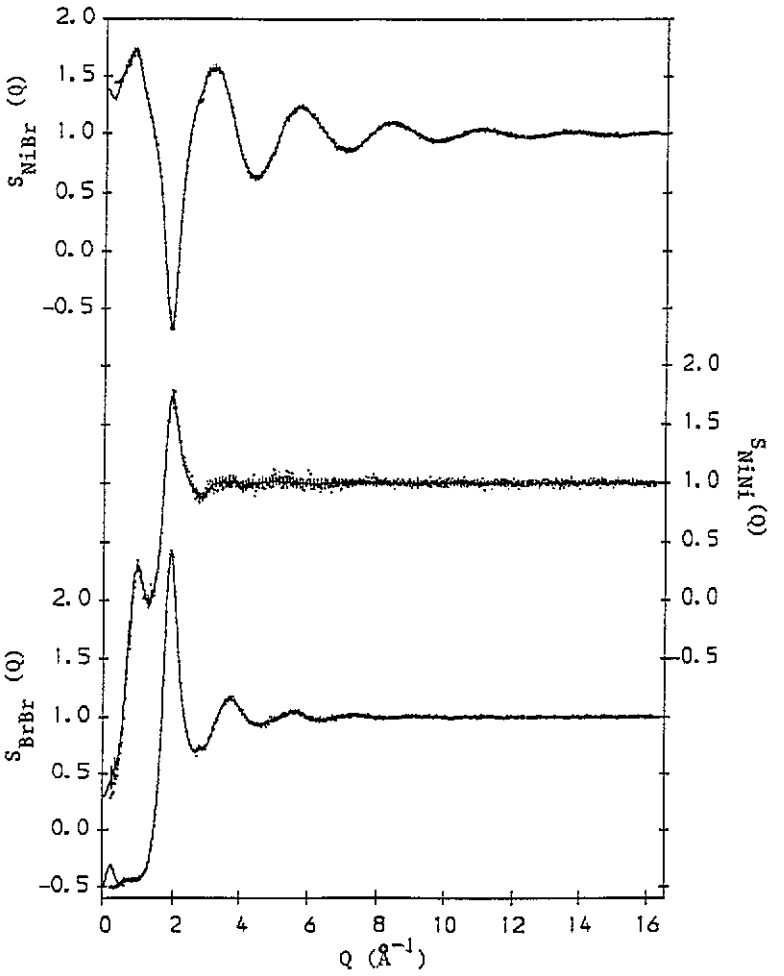

Figure 7. The three partial structure factors for $NiBr_2$ + 9 mol% Ni (●): ——, back transforms of the final $g(r)$-values and show representative error bars.

4. Summary of observations

4.1. NiI_2 + 9 mol% Ni

From a comparison of the two structure factors $S_{II}(Q)$ obtained for the pure salt and the solution, it can be seen that the anion structure is largely unperturbed by the addition of this much excess nickel. The two composite functions $F'(Q)$ in figure 4 also appear to be very similar.

4.2. $NiBr_2$ + 9 mol% Ni

The three partial structure factors for both pure $NiBr_2$ and its solution with 9 mol% Ni are compared in figure 9.

Table 2. Structural parameters in real and reciprocal space for molten $NiBr_2$ + 9 mol% Ni and pure $NiBr_2$.

	$NiBr_2$ + Ni	$NiBr_2$
Ni–Br partial		
Main peak position in $r^2g(r)$	2.45 ± 0.03	2.45 ± 0.03
Main peak position in $g(r)$	2.42 ± 0.02	2.42 ± 0.03
Peak height	≥5.57	≥5.76
Peak width	≤0.41	≤0.41
Depth of first trough	0.55 ± 0.03	0.44 ± 0.04
Coordination number	4.55 ± 0.15	4.62 ± 0.15
Reciprocal space		
Position of 'Coulomb dip' ($Å^{-1}$)	1.90 ± 0.02	1.95 ± 0.02
Depth of dip	−0.68 ± 0.02	−0.78 ± 0.06
Br–Br partial		
Main peak position in $r^2g(r)$	3.91 ± 0.03	3.92 ± 0.05
Main peak position in $g(r)$	3.72 ± 0.02	3.69 ± 0.04
Peak height	1.92 ± 0.02	1.85 ± 0.02
Coordination number	11.7 ± 0.2	11.0 ± 0.3
$\bar{r}_{--}/\bar{r}_{+-}$	1.60 ± 0.02	1.60 ± 0.03
Ni–Ni partial		
Main peak position in $r^2g(r)$	4.3 ± 0.1	3.9 ± 0.2
Main peak position in $g(r)$	3.9 ± 0.1	3.7 ± 0.2
Peak height	1.3 ± 0.1	1.7 ± 0.1
Depth of first trough	0.78 ± 0.06	0.69 ± 0.06
Coordination number	4.6 ± 0.5	5.3 ± 1.0
Reciprocal space		
Main peak position in $S(Q)$ ($Å^{-1}$)	1.95 ± 0.02	1.99 ± 0.02
Main peak height	1.7 ± 0.1	2.3 ± 0.2
Pre-peak position ($Å^{-1}$)	0.95 ± 0.02	0.98 ± 0.02
Pre-peak height	0.89 ± 0.07	0.95 ± 0.1

(i) The anion–anion partial structure factor is again seen to be insensitive to the addition of this concentration of excess nickel. It is observed to be very similar in both real and reciprocal space and the nearest-neighbour coordination number remains at a similar value.

(ii) For the high-Q region ($Q > 3$ $Å^{-1}$) the Ni–Br partial structure factor is also seen to be unchanged upon addition of nickel; the oscillations have the same amplitude and phase up to the maximum Q for this experiment. However, significant changes are observed at lower Q-values. The dip at $Q = 1.95$ $Å^{-1}$ in $S_{NiBr}(Q)$ for pure $NiBr_2$ is both shifted to lower Q and reduced in depth. This dip in S_{+-} is a well established feature of liquids which exhibit charge alternation and occurs for such systems at the same position as the first main peaks in S_{++} and S_{--}. Copestake and Evans (1982) argued that this feature, although indicative of charge ordering, does not necessarily mean coulombic interactions. In real space, the principal peak in $g_{NiBr}(r)$ is unaltered by the presence of excess nickel; it has the same position, height, width, shape and coordination number. The ratio $\bar{r}_{BrBr}/\bar{r}_{NiBr}$ is not changed for the 9 mol% Ni solution. Some filling in of the minimum following the principal peak in g_{NiBr} is observed and the second-neighbour peak is shifted slightly to higher r.

(iii) The only major structural change observed upon addition of excess metal is to be seen in the Ni–Ni partial structure. In S_{NiNi} we observe a significant loss of amplitude;

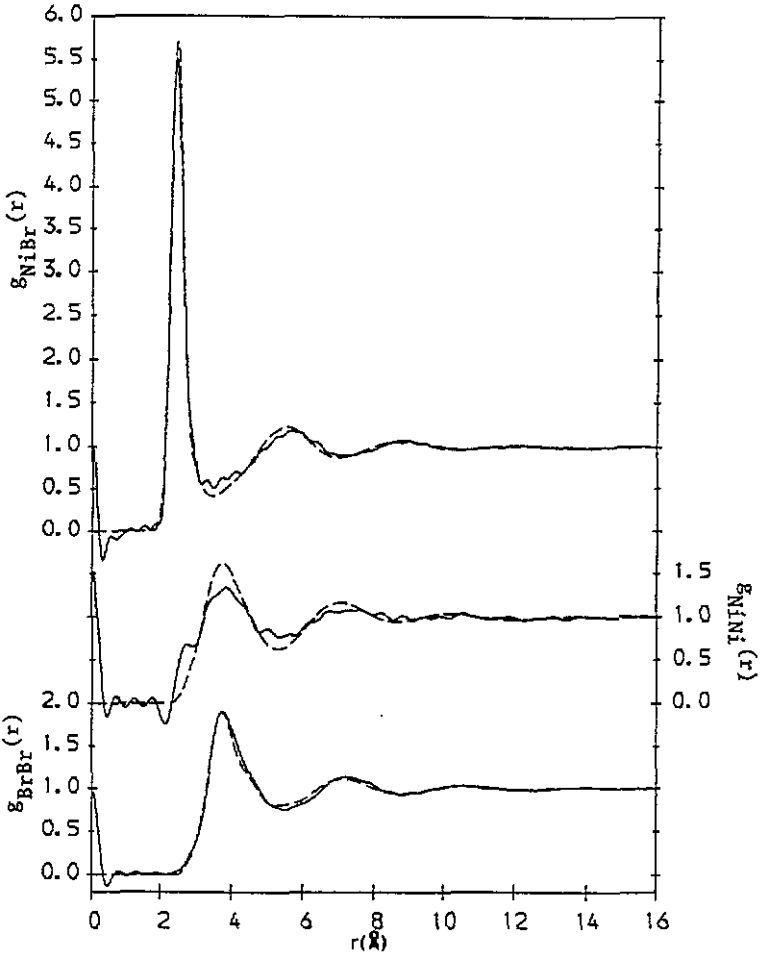

Figure 8. The three partial radial distribution functions for $NiBr_2$ + 9 mol% Ni (——)and pure $NiBr_2$ (–––) (from I).

the principal peak height is reduced and little structure is observed beyond this peak. There is also a shift to lower Q, which corresponds to the shift in the Coulomb dip in S_{NiBr}. The pre-peak observed for pure $NiBr_2$ at $Q = 0.98$ Å^{-1}, which is believed to be indicative of some intermediate-range ordering between the nickel species, is still present for the mixture at a slightly lower Q. Its height appears to be slightly reduced and its width broadened, but this is difficult to quantify since the trough following this peak has been filled in by the shift and broadening of the principal peak. The loss of structure in S_{NiNi} is reflected in real space as an overall reduction in structural ordering of the nickel species. This is seen by the reduction in peak heights and a filling in of the troughs.

5. Discussion

The lack of change in $F'(Q)$ upon addition of excess nickel to NiI_2 suggests that very little change, if any, occurs in the Ni–Ni and Ni–I partial structures, contrary to what

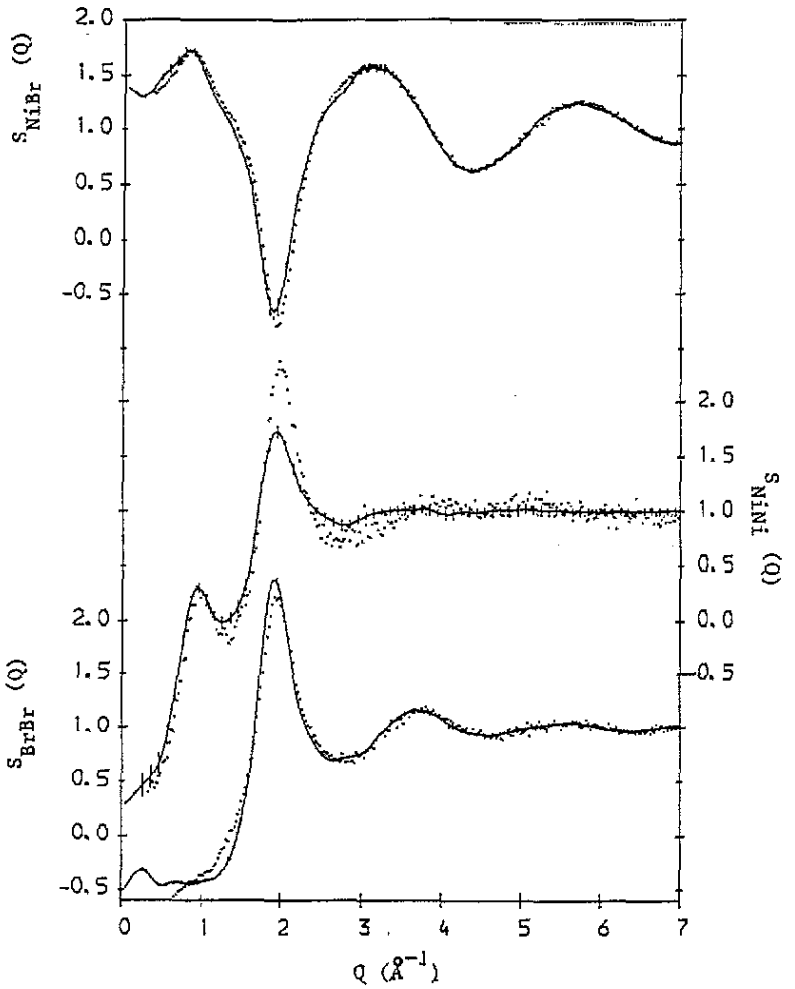

Figure 9. A comparison of the partial structure factors of molten $NiBr_2$ + 9 mol% Ni (——) with those of pure $NiBr_2$ (●) (from I).

one might expect if subhalide complexes were being formed. It should be noted that the Ni–Ni partial is relatively featureless for pure NiI_2, so that changes to this partial, which makes a 35% contribution to $F'(Q)$, may not be readily apparent. However, the formation of complexes involving more than one nickel atom, with well defined Ni–Ni distances, ought to produce observable effects upon $F'(Q)$.

For $NiBr_2$ + Ni, the absence of any new well defined Ni–Br distances excludes the formation of new complexes containing nickel and bromine atoms. Furthermore, the similarity of the principal peak in g_{NiBr} to that of the pure salt indicates that the local configuration of bromine ions around each nickel ion, averaged over the volume of the sample, is not changed. This implies that the excess nickel atoms are occupying vacant tetrahedrally coordinated sites within a largely unperturbed anion structure. The reduction in ordering of the nickel species, seen in the Ni–Ni partial, is at odds with what one would expect to see with the formation of complexes containing more than one nickel atom. If the dissolved nickel is not forming subhalide complexes, then the question

arises of what state the unassociated nickel is in. A number of possibilities will now be discussed.

A study of molten $NiCl_2$ + Ni has been carried out by Johnson *et al* (1958) who, from their observed freezing-point depression and calculated enthalpy of fusion, inferred that the univalent nickel ion is formed according to the equation $Ni + Ni^{2+} \rightarrow 2Ni^{+}$. However, they did not rule out the possibility that nickel exists in solution as atoms.

Considering the first of these possibilities for $NiBr_2$ + Ni. If Ni^+ ions are being formed and are occupying existing tetrahedral sites within the anion structure, then a broadening of the principal peak in g_{NiBr} should be observed on the high-r side owing to the much larger size of this ion. Although no ion size data exist of the rare Ni^+ ion, one would expect a significantly greater radius value than 0.72 Å for the Ni^{2+} ion, whose 4s shell has been emptied. No broadening of this peak is observed. If, however, nickel atoms are present in the melt, then an interatomic Ni–Br distance of 3.1–3.2 Å would be expected from consideration of the atomic and ionic radii. No peak is observed in this region, but a filling in of the trough following the main peak in g_{NiBr} is observed over the region 3.0–4.3 Å. The increased anion–anion separation associated with such an expansion of the local tetrahedral structure would be in the region of 4.9–5.2 Å for $NiBr_2$ and 5.4–5.6 Å for NiI_2, but no increase in the anion–anion distribution functions is observed in these regions. In summary, there is no clear evidence for the existence of nickel species of a lower than normal oxidation state. It is also difficult to see how the presence of such species in existing tetrahedrally coordinated sites could give rise to the observed reduction in the ordering of the nickel species in $NiBr_2$ + Ni. With a filling of vacant sites, one would expect a decrease in the mobility of the nickel species, with a corresponding increase in structural ordering. No published mobility measurements are known for these systems.

The most likely dissolution process for the excess nickel is the formation of doubly charged nickel cations according to the equation $Ni \rightarrow Ni^{2+} + 2e^{-}$. The lack of any substantial change observed for the Ni–Br, Br–Br and I–I partial structures suggests that the excess nickel is occupying similar sites within the anion structures to the nickel already present in the two salts and is therefore of the same size. Such a dissolution results in dissociated mobile electrons in extended states or localized in shallow traps. Thus metallic behaviour is imparted to the melt and the solution belongs to the first 'metallic' category. However, no conductivity measurements are known for either the pure salts or their solutions.

The effect upon the interionic potentials of the presence of conduction electrons is one of screening. Copestake and Evans (1982), using a restricted primitive model, obtained partial structure factors for a molten salt using HNC and MSA calculations based on coulombic and screened coulombic potentials. The short-range screened potential gave similar results to the stronger and longer-range coulombic potential, indicating that the gross structural features of liquids with strong attractive forces between unlike species are insensitive to the exact form of the potentials present. They observed little difference in S_{+-} beyond the first peak, but the 'Coulomb dip' in S_{+-} was reduced in magnitude for the screened potential, indicating a reduction in the level of charge ordering. In addition, the first peak in their $S_{\pm\pm}$ was substantially reduced in height, with a corresponding loss of structural ordering in real space, although this was not pronounced. The changes obtained by the application of screened coulombic interactions are qualitatively the same as those observed here for S_{NiBr} and S_{NiNi}. This supports the possibility that mobile electrons are present in the $NiBr_2$ + Ni mixture. However, the model used by Copestake and Evans assumed equally sized cations and anions with the same charge, which is clearly not the case for these salts. For $NiBr_2$, the cation is

doubly charged and has a diameter of 1.38 Å and a nearest-neighbour separation $\bar{r}_{++}$ of 3.9–4.3 Å, whereas the singly charged anion has a diameter of 3.9 Å and a nearest-neighbour separation $\bar{r}_{--}$ of about 3.9 Å. For NiI_2 the anion diameter is 4.32 Å, compared with a $\bar{r}_{--}$-value of about 3.89 Å. Clearly short-range overlap forces must play a significant role in determining the close-packed anion structures for $NiBr_2$ and NiI_2, which are therefore less susceptible to the effects of coulombic screening. Because of the already structureless form of g_{NiNi} for pure NiI_2 and the minor contribution that this term makes to the reduced structure factor $F'(Q)$, changes in this partial of the kind seen for $NiBr_2$ + Ni may not be visible.

The possible origin of the pre-peak observed for molten salts with relatively small divalent cations is discussed in I and by Allen *et al* (1990), where the evidence for the importance of bond directionality in producing the ordering between tetrahedra is discussed. The mutual Coulomb repulsions between doubly charged cations appears to be less important in producing inter-tetrahedral structural ordering. The pre-peak observed in S_{NiNi} for the $NiBr_2$ + Ni data presented here, when compared with that of the pure salt, is seen to be less sensitive to the addition of excess nickel than the rest of the Ni–Ni structure. This is consistent with the view that its origin is in angle-dependent bonding between cations and polarized anions, rather than Coulomb repulsions between the anions themselves. The pre-peak observed for NiI_2 is unchanged upon addition of excess nickel to this salt.

Acknowledgments

We wish to thank the staff at the ANL (Argonne, IL) and the ILL (Grenoble), in particular Dr J Faber and Mr R Hitterman (ANL) and Dr P Chieux (ILL), for their assistance with the diffraction experiments. Thanks are also due to Dr N D Wood for help in performing these experiments. We are also grateful to Mr P Gullidge of the University of Bristol for assistance in the preparation of the isotopic samples and for the chemical analysis of the $NiBr_2$ + Ni sample. We acknowledge the continued support given to this work by the Science and Engineering Research Council.

References

Allen D A, Howe R A, Wood N D and Howells W S 1990 to be published
Bredig M A and Johnson J W 1960 *J. Phys. Chem.* **64** 1899
Copestake A P and Evans R 1982 *J. Phys. C: Solid State Phys.* **15** 4961
Howells W S 1986 *Rutherford Appleton Laboratory Report* RAL-86-042
Institut Laue–Langevin 1983 *ILL Handbook: Neutron Beam Facilities Available for Users* (Grenoble: Institut Laue–Langevin)
Johnson J W, Cubicciotti D and Kelley C M 1958 *J. Chem. Phys.* **62** 1107
Nachtrieb N H 1974 *Adv. Phys. Chem.* **31** 465
Newport R J, Howe R A and Wood N D 1985 *J. Phys. C: Solid State Phys.* **18** 5249
Sears V F 1984 *Atomic Energy of Canada Ltd. Report* AECL-8490
Waseda Y 1980 *The Structure of Non-Crystalline Materials: Liquids and Amorphous Solids* 1st edn (London: McGraw-Hill)
Wood N D and Howe R A 1988 *J. Phys. C: Solid State Phys.* **21** 3177
Wood N D, Howe R A, Newport R J and Faber J Jr 1988 *J. Phys. C: Solid State Phys.* **21** 669